HTML ABSTRACT + LINKS

Influence of barrier overoxidation and annealing on the inelastic spin-dependent tunneling in AlO_x-based junctions

T. Dimopoulos,[a] Y. Henry, V. Da Costa, C. Tiusan,[b] and K. Ounadjela[c]
IPCMS-GEMME, 23 Rue du Loess, BP43, F-67034 Strasbourg Cedex 2, France

(Presented on 8 January 2004)

The present work reports on the inelastic, spin-dependent tunneling in magnetic junctions with AlO_x barrier and $Co_{50}Fe_{50}$ ferromagnetic (FM) electrodes. The identification of the transport inelastic channels is possible through their distinctive temperature dependencies. For the observed temperature behavior of the magnetotransport properties of the junctions, two spin-dependent, inelastic mechanisms are proposed: assisted tunneling due to interfacial (a) magnons and (b) metallic phonons. Their relative contributions are closely linked to the microstructural properties of the FM metal/oxide interfaces, related to the plasma oxidation of the tunnel barrier and to thermal annealing. © *2004 American Institute of Physics.*
[DOI: 10.1063/1.1667411]

Magnetic tunnel junctions, of the ferromagnet (FM)/insulator (I)/ferromagnet (FM) type, have been the subject of intensive research since large tunnel junction magnetoresistance (JMR) has been measured at room temperature (RT).[1] The JMR effect is the modification of the junction's resistance depending on the relative orientation of the magnetization of the two FMs adjacent to the insulator (tunnel barrier). For simplicity, it is often assumed that the spin polarized electrons tunnel through the tunnel barrier elastically and without modification of the parallel to the layers component of their momentum.[2] Albeit, inelastic transport channels exist and they affect the magnitude, the bias and the temperature dependence of the JMR.[3–5] In this work we will try to reveal the inelastic mechanisms present in as-deposited and annealed AlO_x-based junctions, by means of magnetotransport measurements as a function of the temperature, T.

The multilayers were deposited by magnetron sputtering on Si substrates, with the following stacking sequence: Si/Cr(1.6)/Fe(6)/Cu(30)/$Co_{50}Fe_{50}$(1.5)/Ru(0.8)/$Co_{50}Fe_{50}$(2.5)/Al(x nm; oxidized y sec)/$Co_{50}Fe_{50}$(1)/Fe(6)/Cu(5)/Cr(3) (layer thickness expressed in nm). The tunnel barrier was formed by oxidizing in an Ar/O_2 plasma a presputtered metallic Al film. The thickness, x(nm), and the oxidation time, y(sec), of the Al have been varied as: $(x,y)=(1.2,45)$, $(1.0,40)$, $(0.8,40)$, $(0.6,30)$ (with corresponding multilayers named MTJ1-MTJ4), so as to obtain nearly optimally oxidized, as well as overoxidized barriers. The multilayers were studied as-deposited and after annealing at 300 °C for 1 h. Junctions were patterned by UV lithography, in areas of 3×3 to 100×100 $(\mu m)^2$. Magnetotransport measurements were realized with the standard 4-point technique.

In Fig. 1 we present high resolution transmission electron microscopy (HRTEM) images of the tunnel barrier of the as-deposited multilayers. The AlO_x layer appears to be amorphous, with small and correlated interfacial waviness. For the multilayers employing the thinnest barriers (MTJ3 and MTJ4), structural ambiguities at the bottom FM/oxide interface suggesting oxidation of the FM electrode.

The net magnetic moment, m_{net}^{AAF} of the artificial antiferromagnet (AAF) used as a bottom FM electrode, has been extracted from minor magnetization loops. The values are reported in Table I. Two conclusions can be drawn: (i) m_{net}^{AAF} is reduced for the multilayers with small barrier thickness (MTJ3 and MTJ4). The loss in the magnetic moment is attributed to the oxidation of the top CoFe layer of the AAF, (ii) the loss of the AAF's magnetic moment is partially recovered after thermal annealing, especially for multilayers MTJ3 and MTJ4. This recovery is attributed to the thermodynamically-driven migration of oxygen from the bottom FM electrode to the AlO_x.[6,7]

In Table I we also report the RT JMR values, measured at a constant bias of 5 mV, for the different multilayer stacks. Specifically, the JMR varies from ~25% for MTJ1 and MTJ2 to ~18% for MTJ3 and ~7% for MTJ4. Annealing

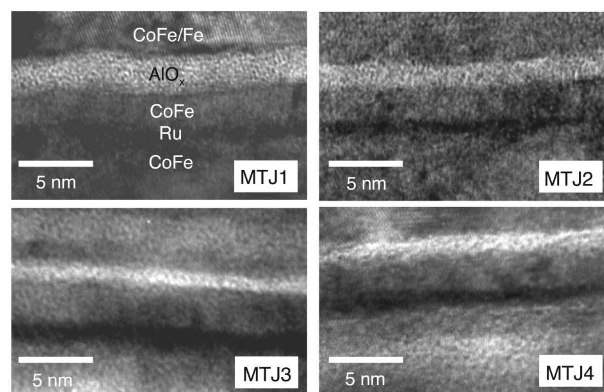

FIG. 1. HRTEM images of the as-deposited multilayers focusing on the AlO_x barrier.

[a]Present address: Siemens AG, Corporate Technology, Erlangen, Germany; electronic mail: theo.dimopoulos.ext@erls.siemens.de
[b]Present address: Laboratoire de Physique des Matériaux, Nancy, France.
[c]Present address: Cypress Semiconductor, San Jose, CA.

 © 2004 American Institute of Physics

Downloaded 15 Feb 2006 to 194.214.217.17. Redistribution subject to AIP license or copyright, see http://jap.aip.org/jap/copyright.jsp

TABLE I. The net magnetic moment of the AAF, the resistance-area product, and the RT JMR for the different as-deposited and annealed multilayers.

Junction	$m_{\mathrm{net}}^{\mathrm{AAF}}$ (10^{-4} emu/cm^2)	$R_P A$ ($k\Omega\times\mu$m^2)	JMR(%)
MTJ1-as-dep.	1909±100	35.6	25.1
MTJ1-ann.	1960±100	25.6	37.5
MTJ2-as-dep.	1963±100	4.16	25.6
MTJ2-ann.	1952±100	5.36	29.1
MTJ3-as-dep.	1834±100	1.24	18.2
MTJ3-ann.	1970±100	···	···
MTJ4-as-dep.	1535±100	0.14	6.9
MTJ4-ann.	1750±100	···	···

enhances the JMR ratio for both MTJ1 and MTJ2 junctions, reaching ~38% and ~29%, respectively. This is consistent with the argument of oxygen migration from the FM electrode towards the AlO_x barrier, that enhances its uniformity and increases the interfacial spin polarization. For every multilayer, the junction resistance–area product and JMR are independent of the junction size.

In Fig. 2 we present the JMR loops for an as-deposited and annealed MTJ1 junction, measured at 6 K and 290 K. The parallel (P) magnetic state is defined at the field value of 12 kOe, which is beyond the saturation field of the AAF for every studied multilayer and temperature. The antiparallel (AP) magnetic state is considered within the antiferromagnetic (AF) plateau of the AAF, at negative field, after the full magnetization reversal of the soft electrode [insets of Figs. 2(a) and 2(b)].

In Figs. 3(a) and 3(b) we present the temperature dependence of the junction conductance G_γ, where γ=P, AP, normalized to its value at 6 K. For all junctions we obtain a relatively weak, insulatinglike $G(T)$ variation, suggesting that tunneling is the dominant transport mechanism.[8,9]

The change of the average junction conductance between 6 and 290 K varies between 20% and 35%. Such a large increase cannot be explained by the T dependence of the elastic conductance due to the smearing of the Fermi distribution. Indeed, this can reach only a few percent (2%–5%), depending on the barrier parameters (the increase is larger for thick and small height barriers). We therefore consider alternative, temperature-dependent, transport channels. A possiblity is spin-independent, assisted tunneling via hopping of electrons to N impurity states inside the barrier.[10] Its temperature dependence $G^{\mathrm{hop}}\sim T^{\nu}$, where $\nu=N-[2/(N+1)]$, arises from the phonon absorption or emission at the transition from one localized state to the next.[11] At least two localized states are needed in order to obtain temperature dependence of the conductance (since for $N=1$, $\nu=0$). Hopping via multiple localized states is rather unlikely, considering the small thickness of the barriers under study yet, it cannot be excluded. Nevertheless, since the impurity-assisted tunneling is spin independent, it cancels out in the quantity $\Delta G=G_{\mathrm{P}}-G_{\mathrm{AP}}$, for which the temperature behavior is depicted in Fig. 3(c) $\Delta G(T)$, therefore, integrates only spin-dependent channels.

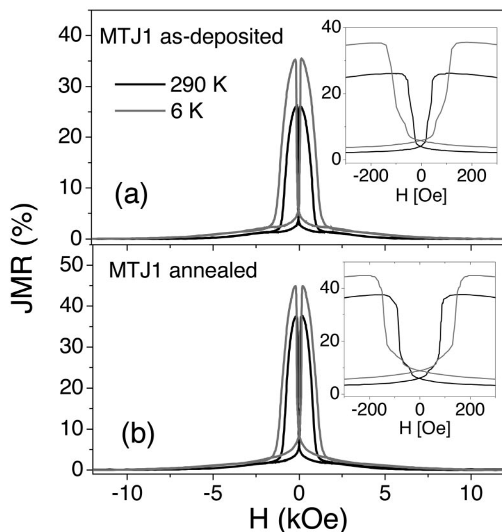

FIG. 2. JMR loops at 6 K and 290 K for (a) an as-deposited and (b) annealed MTJ1 junction. The insets zoom in the small field region, at the AF plateau of the AAF, where the AP state is defined.

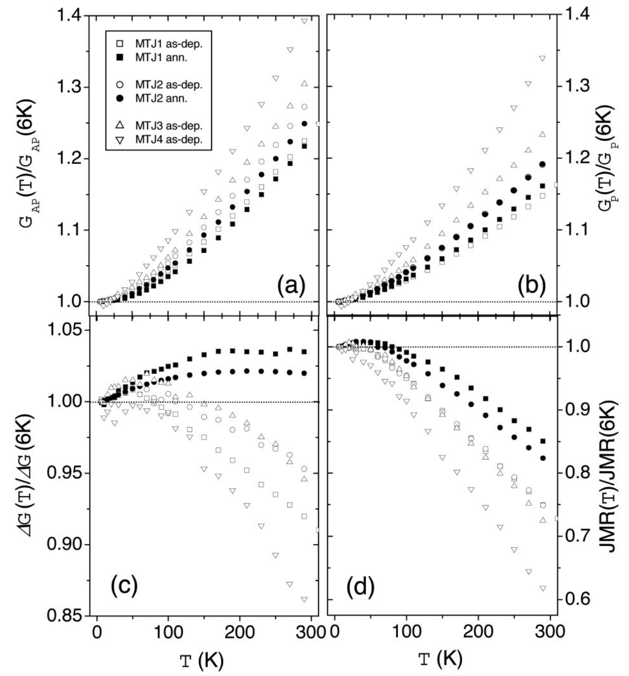

FIG. 3. The temperature dependence of (a) the AP conductance G_{AP}, (b) the P conductance G_{P}, (c) the quantity $\Delta G=G_{\mathrm{P}}-G_{\mathrm{AP}}$, and (c) the JMR. All quantities are normalized to their value at $T=6$ K. The bias voltage was set to 5 mV for all measurements.

For the as-deposited junctions, (i) the increase of G_γ with T, depicted in Figs. 3(a) and 3(b), is larger for the thinner barriers, for which the oxidation of the bottom FM electrode is more pronounced, (ii) ΔG is a decreasing function of T beyond $T\approx 50$ K. This is consistent with a spin–flip transport mechanism which contributes more to the AP conductance than to the P conductance. Indeed, the oxidation of the bottom FM electrode reduces its interfacial Curie temperature, T_C. This facilitates the absorption or emission of $2D$ magnons by electrons, which scatter inelastically and flip their spin direction. The larger is the oxidation of the FM electrode, the stronger is expected to be the magnon-assisted tunnel conductance and the mixing of the two spin channels.

Downloaded 15 Feb 2006 to 194.214.217.17. Redistribution subject to AIP license or copyright, see http://jap.aip.org/jap/copyright.jsp

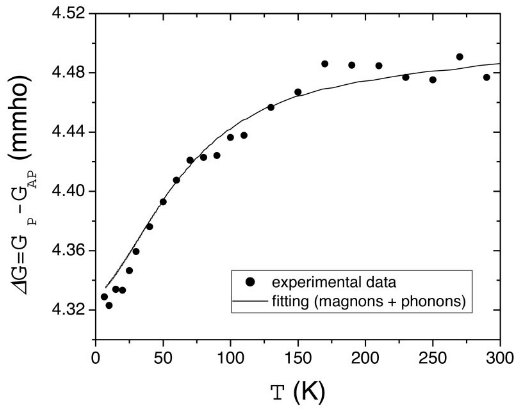

FIG. 4. Fitting of the experimental $\Delta G(T)$ data of an annealed MTJ1 junction, with the model that takes into account magnons and phonons of the FM electrodes.

Although the negative sign of the $\Delta G(T)$ clearly suggests a spin–flip process, other inelastic channels may be concealed by the dominant spin–flip contribution.

Indeed, for the annealed junctions, ΔG is increasing as a function of T. This clearly suggests an additional spin-conserving, tunnel-assisting mechanism. Moreover, annealed junctions exhibit reduced temperature variation of the AP conductance and increased temperature variation of the P conductance, compared to the corresponding as-deposited ones [Figs. 4(a) and 4(b)]. These can be explained by the combined effect of two transport contributions. One arises from the spin–flip, magnon-assisted tunneling and the other from spin-conserving, phonon-assisted tunneling. For the annealed junctions the relative contributions of the two channels are modified compared to the as-deposited ones, giving rise to a different behavior of $\Delta G(T)$. As mentioned before, upon annealing the oxygen diffuses from the bottom FM electrode towards the AlO_x barrier, enhancing the interfacial T_C. This would decrease the electron-magnon scattering. On the other hand, the phonon energy spectrum of the FM/oxide interfaces will be lowered. For example, the Co–O stretching mode is situated at ~ 60 meV and the Al–O stretching mode at ~ 110 meV.[12] Due to the oxygen transfer after annealing, metallic phonons with lower energy spectrum can be easier easily activated at the FM/oxide interface, giving rise to stronger spin-conserving scattering For comparison, the energy spectrum of the phonon density of states of the $Co_{92}Fe_8$ alloy ranges from 5 to 35 meV,[13] while room temperature corresponds to ~ 25 meV. It is thus likely that metallic phonon modes are thermally excited, as in the case of magnons.

The zero-bias, phonon-assisted conductance as a function of T writes[5]

$$G_\gamma^p(T) = \frac{2\pi e^2}{\hbar} A^\gamma 3\kappa \left(\frac{T}{\Theta_D}\right)^4 \int_0^x dx \frac{x^3}{e^x - 1}, \quad x = \frac{\Theta_D}{T}, \quad (1)$$

while for the magnon-assisted, spin–flip contribution we have[4]

$$G_\gamma^m(T) = \frac{-2\pi e^2}{\hbar} B^\gamma |T_J|^2 \frac{2S(S+1)}{3} \frac{T}{T_C} \ln(1 - e^{(-T_{lc}/T)}). \quad (2)$$

Here κ is a constant entering in the matrix element of the electron–phonon interaction: $P = \kappa(T_{\mathrm{ph}}/\theta_D)$.[14] Θ_D is the Debye temperature and T_{ph} is the phonon temperature. $|T_J|^2$ is the spin–flip matrix element and S is the interfacial spin. T_{lc} corresponds to the lower cut-off energy for the magnons.[4] $A^{\mathrm{P}} = B^{\mathrm{AP}} = \rho_M^2 + \rho_m^2$ and $A^{\mathrm{AP}} = B^{\mathrm{P}} = \rho_M \rho_m$, where $\rho_M(\rho_m)$ is the electronic density of states for majority (minority) electrons of the FM electrodes. Assuming that $T_{lc} \ll T$, Eq. (2) becomes

$$G_\gamma^m(T) = \frac{2\pi e^2}{\hbar} B^\gamma |T_J|^2 \frac{2S(S+1)}{3} \frac{T}{T_C} \ln T. \quad (3)$$

In Fig. 4 we present the fit of the experimental $\Delta G(T)$ curve of the annealed MTJ1 junction to the model that takes into account electronic scattering with phonons [Eq. (1)] and magnons [Eq. (3)] at the FM electrode interfaces. For the fitting we take $T_C = 1200$ K, $\Theta_D = 370$ K and $S = 3/2$ for the CoFe electrodes. The direct tunneling term corresponds to the value $\Delta G(6\mathrm{K}) = (2\pi e^2/\hbar)(A^{\mathrm{P}} - A^{\mathrm{AP}})|T_d|^2 = 4.33 \times 10^{-3}$ mho, where $|T_d|^2$ is the direct tunneling matrix element. The fitting of the experimental data yields $K^p = (2\pi e^2/\hbar)(A^{\mathrm{P}} - A^{\mathrm{AP}}) 3\kappa = 2.723 \times 10^{-3}$ mho and $K^m = (2\pi e^2/\hbar)(B^{\mathrm{P}} - B^{\mathrm{AP}})|T_J|^2 = -1.702 \times 10^{-4}$ mho. From these parameters we obtain $|T_d|^2/|T_J|^2 = 25$ and $|T_d|^2/\kappa = 4.8$. Consequently, the direct tunneling matrix element is considerably larger compared to the magnon and phonon-assisted tunnel matrix elements, as expected.

As pointed out by Bratkovsky,[5] phonon-assisted tunneling lowers the detrimental effect of the spin–flip magnon scattering on the JMR. Indeed, as we can see in Fig. 4(d) the JMR decreases less with temperature for the annealed junctions, while the maximum decrease of JMR is measured for the overoxidised, as-deposited junctions.

In conclusion, we have demonstrated that magnon-assisted tunneling is not adequate to describe the *zero-bias*, temperature dependence of the conductance and JMR. In annealed junctions, for which the magnon transport contribution is reduced, a spin-concerving transport mechanism is revealed. This most possibly arises from the electron scattering with phonon modes of the FM junction electrodes.

[1] J. S. Moodera, L. R. Kinder, T. M. Wong, and R. Meservey, Phys. Rev. Lett. **74**, 3273 (1995).
[2] J. C. Slonczewski, Phys. Rev. B **39**, 6995 (1989).
[3] J. S. Moodera, J. Nowak, and R. J. M. van der Veerdonk, Phys. Rev. Lett. **80**, 2941 (1998).
[4] S. Zhang, P. M. Levy, A. C. Marley, and S. S. P. Parkin, Phys. Rev. Lett. **79**, 3744 (1997).
[5] A. M. Bratkovsky, Appl. Phys. Lett. **72**, 2334 (1998).
[6] M. Sato, H. Kikuchi, and K. Kobayashi, Fujitsu Sci. Tech. J. **34**, 204 (1998).
[7] R. C. Sousa, J. L. Sun, V. Soares, P. P. Freitas, A. Kling, M. F. Silva, and J. C. Soares, J. Appl. Phys. **85**, 5258 (1999).
[8] *Tunnelling Phenomena in Solids*, edited by E. Burstein and S. Lindqvist (Plenum, New York, 1969).
[9] U. Rudiger, R. Calarco, U. May, K. Samm, J. Hauch, H. Kittur, M. Sperlich, and G. Guntherodt, J. Appl. Phys. **89**, 7573 (2001).
[10] C. H. Shang, J. Nowak, R. Jansen, and J. S. Moodera, Phys. Rev. B **58**, 2917 (1998).
[11] L. I. Glazman and K. A. Matveev, Zh. Eksp. Teor. Fiz. **94**, 332 (1988).
[12] X. F. Han, J. Murai, Y. Ando, H. Kubota, and T. Miyazaki, Appl. Phys. Lett. **78**, 2533 (2001).
[13] S. M. Shapiro and S. C. Moss, Phys. Rev. B **15**, 2726 (1977).
[14] A. B. Migdal, Sov. Phys. JETP **34**, 996 (1958).

Downloaded 15 Feb 2006 to 194.214.217.17. Redistribution subject to AIP license or copyright, see http://jap.aip.org/jap/copyright.jsp